DE GRUYTER OPEN
www.czasopisma.pan.pl PAN www.journals.pan.pl
PAN
DOI: 10.1515/igbp-2016-0004 PAPERS on GLOBAL CHANGE, 23, 37–57, 2016

SYMPTOMS AND DRIVING FACTORS OF CONTEMPORARY EARTH WARMING AND PROJECTIONS FOR THE FUTURE

JOANNA WIBIG
Department of Meteorology and Climatology
Faculty of Geographical Sciences, Łódź University
90-139 Łódź, Narutowicza 88, Poland
e-mail: joanna.wibig@geo.uni.lodz.pl

ABSTRACT: This paper outlines the symptoms of contemporary global warming, reviews its possible driving factors and presents some projections for future. Key among the symptoms are those related to temperature, with the increase in average global temperature since 1880 now reaching a value of 0.85°C. While warming has encompassed almost the whole world, the high latitudes have warmed more than the low, and maximum temperature has increased more than average temperature. Warming has been causing sea level rise, thanks to both the thermal expansion of warming water and the melting of ice on land.

The other consequence of warming is a change in precipitation pattern, manifesting itself in higher precipitation in certain parts of the world (generally at low and high latitudes), but also lower precipitation in other parts (mainly the Tropics); as well as in changes in the intraannual course characterising precipitation (with more falling in winter and less in summer), and in the frequency and intensity of rainfall (more intense heavy-precipitation events and higher variability where the frequency of precipitation is concerned).

Among the possible driving factors, the most important are those related to the increase of CO_2 and mixing ratios of other greenhouse gases in the troposphere. Land-use changes and emissions of aerosols to the atmosphere also exert a major impact on temperature. These are mainly anthropogenic factors. While natural drivers also modulate the climate markedly, they tend to warm and cool the globe alternately, stepping up warming when they are in a warming phase, but slowing down or even offsetting warming during a cooling phase.

Projections for the future are entirely dependent on socio-economic scenarios of future development. All the (economically) realistic scenarios point to a continuation of the warming trend, with a further intense sea-level rise and precipitation changes, albeit with the rate of change varying in line with the rate of increase in concentrations of the greenhouse gases. The realistic range of values for average rise in global temperature is between 2 and even 6 degrees Celsius.

KEY WORDS: global warming, anthropogenic drivers, natural drivers, socio-economic scenarios, projections for the future.

INTRODUCTION

In its Third Assessment Report of 2001, the Intergovermental Panel on Climate Change (further IPCC) forecast that, by the end of the 21st century, the world could be hotter by three degrees Celsius, with a considerably possibility that the size of the increase might even reach six degrees. In turn, in the Foreword to Robert Henson's book titled *The Rough Guide to Climate Change* (Henson 2008), James Lovelock writes that "*Three degrees does not sound like much, but it represents a rise in temperature comparable with the global heating that occurred between the last Ice Age, some 15 000 years ago, and the warmth of the eighteen century*". Fifteen years later, with the IPCC's Fifth Assessment Report (AR5), – IPCC (2013) now published, there seems to be a real risk of even greater warming. The aim of this paper is thus to summarise briefly what is known about the symptoms of global warming, as well as the reasons for it, and the prognoses and projections associated with it. Specifically, the paper is divided into consecutive parts presenting the main symptoms of warming, and the driving factors, as well as certain projections for the future.

SYMPTOMS

The last IPCC Report (IPCC 2013) states "***Warming of the climate system is unequivocal, and since the 1950s, many of the observed changes are unprecedented over decades to millennia. The atmosphere and ocean have warmed, the amounts of snow and ice have diminished, and sea level has risen.***"

Climate change research is based on observations of the climate system. These can entail direct *in-situ* measurements, or remote sensing from satellites or other platforms. *In situ* measurements cover periods ranging between about two centuries, in the case of Europe, to 60–70 years in less-populated or uninhabited regions like Antarctica or Greenland. Satellite measurements are available for the period since the end of the 1970s. Contemporary climate warming covers the period since the turn of the nineteenth and twentieth centuries.

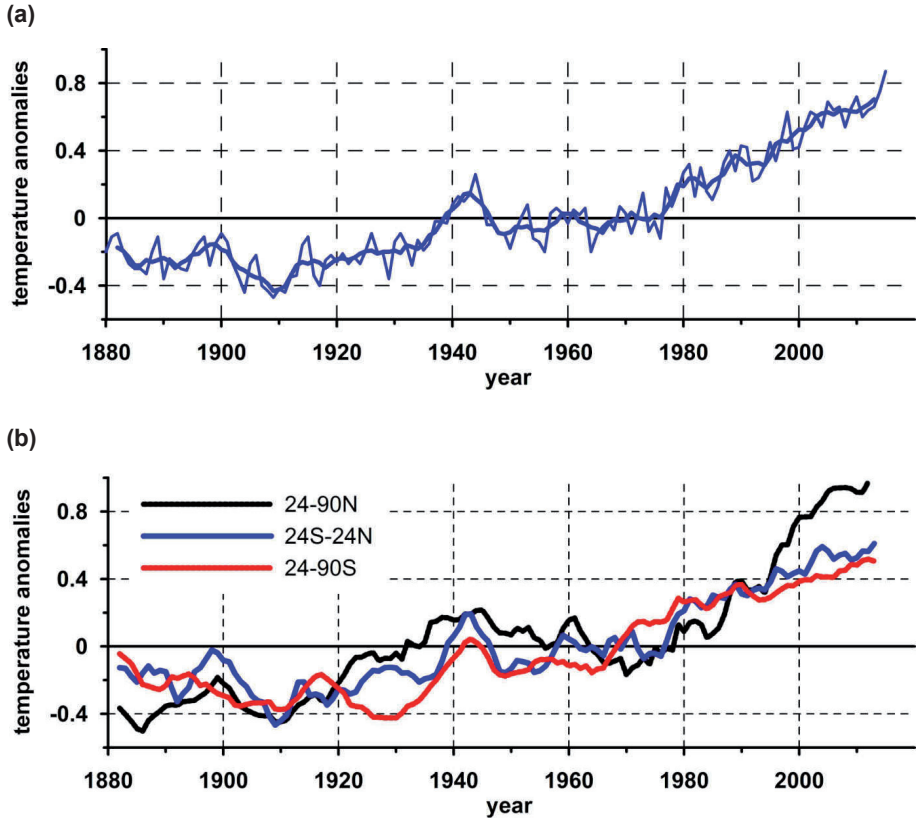

Figure 1. Global annual average temperature anomalies (°C): annual averages and 5-year smoothed values. 5-year smoothed averaged temperature for the Northern Hemisphere (24°N–90°N), the Tropics (24°S–24°N) and the Southern Hemisphere (24°S–90°S). All values are anomalies in comparison with the 1951–1980 reference period. Data are taken from the NASA GISS Surface Temperature Analysis (Hansen *et al.*, 2010, downloaded from data.giss.nasa.gov/gistemp/)

The globally averaged surface temperature showed a warming trend of 0.85°C (0.65–1.06) over the period 1880–2012 (Fig. 1a). This warming was not uniform, however, but proceeded via a first phase lasting from the 1910s through to the 1940s, and a second, stronger phase lasting from the 1970s through to the present. These two phases are more apparent in the Northern Hemisphere (Fig. 1b).

The pace of warming has speeded up lately, with each of the last three decades being warmer than any preceding once since the beginning of the contemporary warming (IPCC 2013). Because more complete observations covering the whole Earth have been accessible since the mid-twentieth century, we can be fully confident that the warming occurring since that time is real. Until recently, 1998 was the warmest year to feature in the instrumental record for global surface temperatures, but last year (2015)

emerged as even warmer than that. Both of these years were in fact ones with strong El-Niño events.

The aforementioned fact that the temperature of the Northern Hemisphere has increased more rapidly can be linked with the presence of most land areas there, as opposed to in the Southern Hemisphere, and in turn to the far faster increase in temperature over land as opposed to over the ocean.

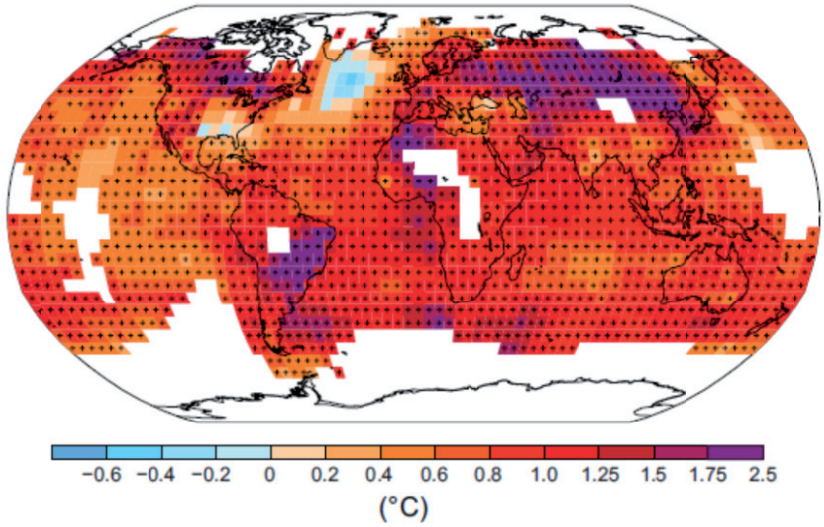

Figure 2. Map of the observed surface temperature change in the years 1901 to 2012, as derived from the temperature trend assessed using linear regression. Trends have been calculated where data availability permits a robust estimate (grid boxes with more than 70% of data, and more than 20% of data in the first and last decades). Other areas are white. Grid boxes for which the upward trend is significant at the 10% level are indicated using a plus sign (+) (after SPM1b, in IPCC, 2014)

Figure 2 makes it clear that warming is evident almost everywhere on Earth, albeit with the strongest trend (exceeding 2°C in some places) characterising the northern part of the Northern Hemisphere. There are also regions in which the temperature has been decreasing, with the most prominent such example of cooling relating to the northern Atlantic close to south-eastern margins of Greenland. It is possible that this cooling reflects a slowdown in the Atlantic Ocean Circulation (Archer, Rahmstorf 2010).

Global rises in sea level (Fig. 3) are an important consequence of warming. According to the last IPCC report (IPCC 2013) the global average sea level rise was of 1.7 ± 0.2 mm/year between 1901 and 2010. However, the rate has accelerated recently, to 2.0 ± 0.3 in the 1971–2010 period, and even 3.2 ± 0.4 between 1993 and 2010. There are two main causes of this rise: the thermal expansion of warming water, and the melting of ice on land. The latter phenomenon is mainly affecting Greenland and the Antarctic, given the presence of the greatest amounts of land ice in those two

places. However, mountain glaciers have also been retreating, and this is a matter of some importance in that these glaciers retain winter precipitation, releasing water slowly in spring and summer, and thus providing fresh water for the inhabitants of submontane regions, who use it for drinking and agriculture, as well as supplying the natural vegetation.

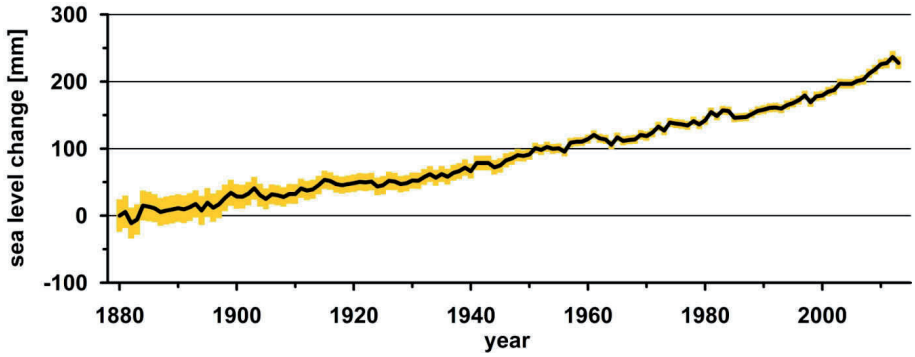

Figure 3. Sea level rise and its 5–95% confidence range
(data from Commonwealth Scientific and Industrial research Organization, http://www.cmar.csiro.au/sealevel/sl_data_cmar.html)

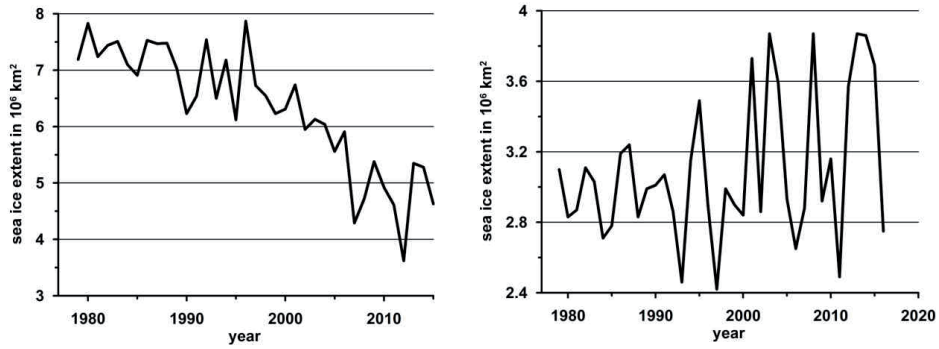

a) Arctic September b) Antarctic February

Figure 4. The area covered by sea ice in the month of minimum annual ice coverage: a) the Arctic in September, b) the Antarctic in February. Data from the National Snow and Ice Data Center (http://nsidc.org/data/g02135.html)

Another effect of warming is the melting of sea ice, which has no consequences for sea level (given that ice dipped in water has the same volume as the water after this ice has melted), but does produce a strong warming feedback, as the albedo of water is much lower than that of ice, with the result that light previously reflected from sea ice is absorbed by water once that ice has melted, thereby warming that water additionally. Over the Northern Hemisphere there is an evident downward trend for the extent of sea ice, which reaches a minimum in early autumn (mid-September). According to the last

IPCC report (IPCC 2014), the mean annual extent of Arctic sea ice decreased over the 1979–2012 period at rates between 0.45 and $0.51 \cdot 10^6$ square kilometers per decade. At the same time, the extent of sea ice in summer (the sea ice minimum) has decreased by between 0.73 and $1.07 \cdot 10^6$ square km per decade. Sea ice around Antarctica has in fact been increasing in area over recent decades. The IPCC report (IPCC 2014) assesses this increase at $0.13–0.20 \cdot 10^6$ square km per decade over the above period. This has been accompanied by the warming of the Southern Ocean. Zhang (2007), IPCC (2013) explain this by reference to a combination of more frequent cyclonic winds around Antarctica and changes in ocean circulation. In the waters around Antarctica there is a thin layer of cold water near the surface and warmer water below. Water from the warmer layer rises to the surface, melting the ice. However, more precipitation (in either the liquid or solid phases) occurs over warmer sea, so this water freshens and thus becomes lighter than the salty water below. This hinders the transport to the surface of heat from the deeper, warmer layer, and hence also the melting of sea ice.

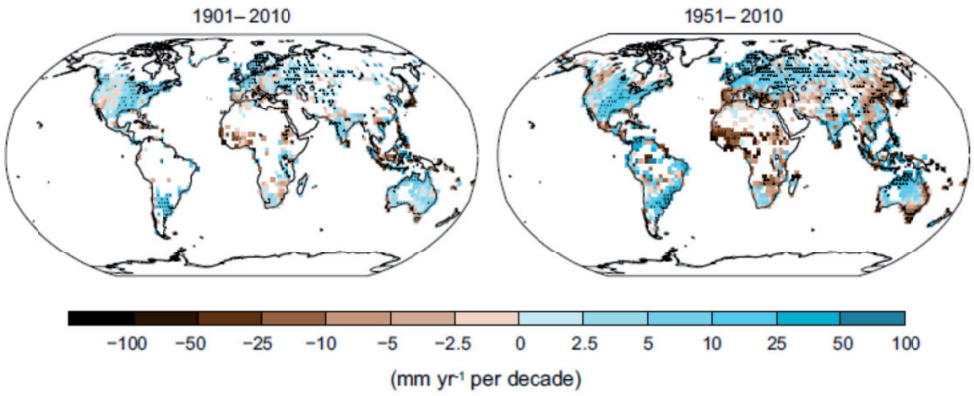

Figure 5. Maps of observed precipitation change from 1901 to 2010 and from 1951 to 2010 (trends in annual accumulation calculated using the same criteria as in Figure 4; after SPM2, in IPCC, 2014)

In the case of precipitation the long-term changes are seen to be much more limited than the year-to-year variability, with trends emerging as both positive (e.g. in mid-latitude land areas of the Northern Hemisphere) and negative (e.g. in the Mediterranean Basin).

"*Changes in many extreme weather and climate events have been observed since about 1950. Some of these changes have been linked to human influences, including a decrease in cold temperature extremes, an increase in warm temperature extremes, an increase in extreme high sea levels and an increase in the number of heavy precipitation events in a number of regions*" (IPCC 2014).

As in the case of means for climate, changes relating to extremes of temperature are expressed much more clearly than those involving precipitation. Numbers of cold

days and nights have decreased, while there have been increases in numbers of warm and hot days, as well as warm nights. The frequency of occurrence of heat waves is also greater now, increasing the level of hazard posed to public health, and ultimately also the mortality risk.

REASONS

ANTHROPOGENIC DRIVERS

"*It is unequivocal that anthropogenic increases in the well-mixed greenhouse gases (WMGHGs) have substantially enhanced the greenhouse effect, and the resulting forcing continues to increase*" (IPCC 2013).

Changes in the environment introduced by human beings – mainly thanks to emissions of various chemical compounds to the atmosphere and land-use changes – have exerted a strong influence on the amount of energy absorbed by the Earth and its atmosphere, with the planet's overall radiation balance affected as a consequence. In assessing the impact of various mechanisms on this balance, use is made of the concept of radiative forcing (further RF), with attendant mechanisms usually divided into three main groups (Fig. 6). The first of these comprises all the effects related to greenhouse gases. The radiative impacts of aerosols are in turn considered in the second group, while the third involves all the effects relating to changes in land use. In this concept, RF is the net change in the downward radiative flux due to specific perturbation. This change is assessed while keeping surface and tropospheric temperature as well as water vapour and cloud cover unperturbed, but allowing for radiative equilibrium adjustment of the stratospheric temperature. RF is expressed in watts per square meter. As it is a net change, it is presented as a difference between the present-day value and the pre-industrial value. This second date is usually fixed at 1750 – as year in which the industrial era is notionally taken to have begun. In response to the net change in RF, the equilibrium global mean temperature alters, while the relationship between RF and change in global temperature (ΔT) is expressed by reference to the climate sensitivity parameter (λ):

$$\Delta T = \lambda \cdot RF.$$

Greenhouse gases can be further divided into the well-mixed greenhouse gases (WMGHGs) and the near-term climate forcers (NTCFs). The well-mixed gases are long-lived ones, in that the time of retention in the atmosphere exceeds that necessary for mixing in the troposphere, with the result that concentrations are relatively uniform around the globe, and need measuring at just a few representative sites. Concentrations nevertheless vary to some extent, in proximity to the so-called sources and sinks, and small hemispheric gradients can even come into existence as a result. CO_2, N_2O, CH_4, SF_6 and many halogenated species come within the WMGHGs. In contrast, the NTCFs are short-lived compounds with atmospheric lifetimes of less than a decade, and non-

uniform concentrations in the troposphere. The NTCFs include short-lived halogenated species, but also methane (which is included among the WMGHGs as well), plus aerosols, and ozone and its precursors. These gases do not accumulate in the atmosphere over time scales extending for decades or longer.

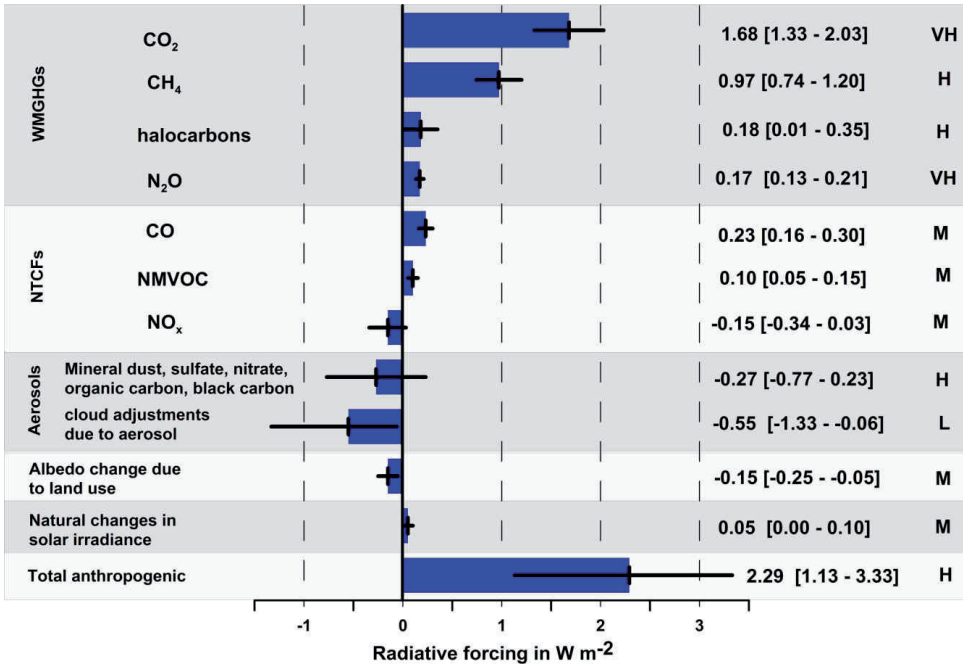

Figure 6. Radiative forcing assessment in 2011 relative to 1750

The best estimates and their uncertainty intervals are shown in black, while the relevant values are given on the right. The confidence levels associated with the net forcing are also given: (VH – very high, H – high, M – medium, L – low). Figure based on the SPM5 figure from WG1AR5, IPCC 2013.

The RF of WMGHGs can be determined directly by observation, given that concentrations of these gases in the atmosphere are roughly uniform and so can be determined from measurements at just a few sites. Values for the pre-industrial era are taken from air bubbles trapped in polar ice. The four most important gases are found to be CO_2, CH_4, halocarbons (most importantly CFC-12 or dichlorodifluoromethane), and NO_2. Halocarbons are entirely of anthropogenic origin and so they were not present in the atmosphere in the pre-industrial era.

The tropospheric mixing ratio of CO_2 has increased from 278 ppm (276–280) in 1750 to 407.7 ppm in May 2016, being 390.5 in 2011 (390.3–390.7) when the RF values for AR5 IPCC were calculated (IPCC, 2013). In the modern era continuous measurements of CO_2 have been conducted since 1958 at the Mauna Loa mountain site on Hawaii. The rate of increase in the mixing ratio for CO_2 is seen to be rising steadily

(Fig. 7), with the rate of increase close to 3 ppm per year at present. In AR5 (IPCC, 2013), the RF resulting from the CO_2 increase between 1970 and 2011 was given as 1.68 (1.33–2.03) Wm^{-2} (Fig. 6). A changing mixing ratio for CO_2 can also influence climate through its impact on lapse rate, clouds, plant physiology (together with transpiration) and vegetation distribution (Andrews *et al.* 2012, IPCC 2013).

The globally averaged surface concentration of methane (CH_4) increased from 722 ± 25 ppb in 1970 to 1840.6 as of February 2016, while being at a level of 1803 ± 2 ppb in 2011 (Fig. 8), when the RF assessment for AR5 was made (IPCC 2013). The atmospheric lifetime of methane is much shorter than that of CO_2, and emissions

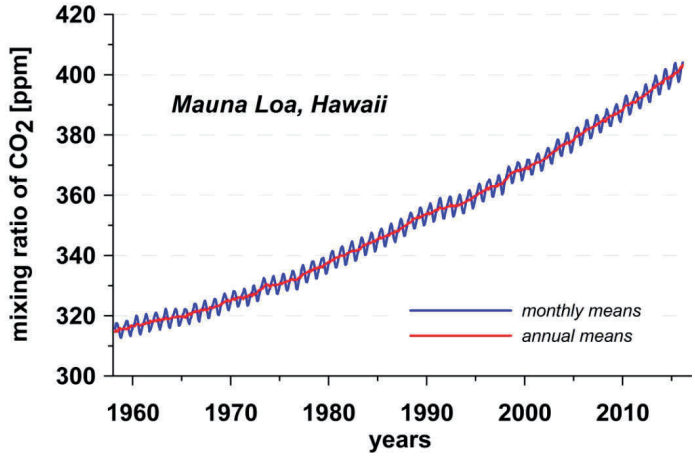

Figure 7. The mixing ratio for CO_2 in the atmosphere, as measured at the Mauna Loa Observatory (data from the Earth System Research Laboratory, www.esrl.noaa.gov/gmd/ccgg/trends/)

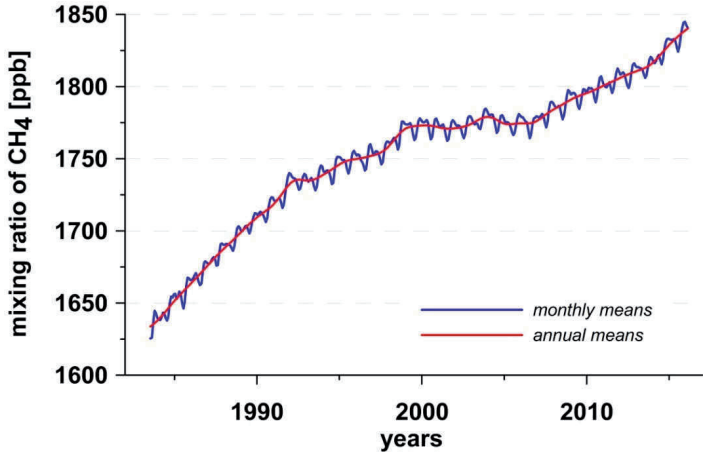

Figure 8. The globally averaged surface mixing ratio for CH_4 in the atmosphere (data from the Earth System Research Laboratory, www.esrl.noaa.gov/gmd/ccgg/trends_ch4/)

are not distributed uniformly, so local mixing ratios noted for CH_4 can differ significantly from the globally averaged value (Dlugokencky *et al.* 2015). The RF for the CH_4 increase between 1750 and 2011, as given in AR5 (IPCC 2013) was 0.97 (0.84–1.20) Wm^{-2} (Fig. 6). CH_4 can influence climate through its direct impact on downward radiation flux, but also through an impact on the CO_2 mixing ratio, stratospheric water vapour content, ozone, the lifetime of some halogenated species and sulphate aerosols.

The concentration of nitrous oxide increased from 270 ± 7 ppb in 1750 to 328.6 ppb in February 2016, being at 324.2 ± 0.1 in 2011, when the RF due to it was assessed for AR5 (IPCC 2013). The RF for the N_2O increase between 1750 and 2011 was given in AR5 (IPCC 2013), the value being 0.17 (0.13–0.21) Wm^{-2}.

Halocarbons are new components in the atmosphere, as they are entirely of anthropogenic origin. There are tens of compounds in the halocarbon family, but the four that are most abundant (with a cumulative RF accounting for about 85% of a total halocarbon input assessed in 2011 at 0.360 (0.324–0.396) Wm^{-2}) – IPCC (2013) are CFC-12 (dichlorodifluoromethane, RF = 0.17), CFC-11 (trichlorofluoromethane, RF = 0.062), HCFC-22 (chlorodifluoromethane, RF = 0.045) and CFC-113 (trichlorofluoroethane, RF = 0.022). The mixing ratio of all halocarbons is very low and is given in ppt (particles per trillion).

Ozone occurs in the atmosphere in the two layers known as the troposphere and the stratosphere. Tropospheric ozone is formed by photochemical reactions from precursor species of natural and anthropogenic origin. Its lifetime is very short, so it does not accumulate in the troposphere, and concentrations vary in time and space. This acts as a greenhouse gas in the troposphere, so its RF is positive and is assessed at 0.40 (0.20–0.60) Wm^{-2}. The high uncertainty results from intermodel differences (IPCC 2013). Ozone in the troposphere reduces the productivity of plants, thus affecting the natural uptake of CO_2. The amount of tropospheric ozone is increasing due to increased emissions of its precursors of anthropogenic origin. The opposite is true in the stratosphere. Due to anthropogenic emission of ozone-depleting species (ODS), the amount of ozone in the stratosphere is decreasing. This has an impact in ensuring a greater flux of shortwave radiation reaching the troposphere, as well as a smaller amount of longwave radiation coming back to the troposphere. The net RF seems to be negative and equals –0.05 (–0.15–0.05) Wm^{-2}, though because of the major uncertainty, there is a small possibility that it is positive.

Water vapour reaches the stratosphere via flux from the tropical troposphere, incidental injections from volcanic eruptions and *in situ* chemical production from the oxidation of methane and hydrogen. All these processes were natural, but some are enhanced by anthropogenic effects. There is also additional flux from aircraft. The RF associated with the anthropogenic increase in stratospheric water vapour is assessed at 0.07 (0.02–0.12) Wm^{-2}, and is positive.

Atmospheric aerosol is a mixture of solid and liquid particles suspended in the atmosphere. These can be of natural or anthropogenic origin. Their life time is very short, usually below two weeks in the troposphere and up to 3 years in the stratosphere. Anthropogenic aerosol is shown to have been cooling the Earth's atmosphere. Overall, the effects aerosol exerts on radiation can be divided into the direct aerosol effects, the

cloud albedo effects and the black carbon effects. Direct effects include all the processes of scattering and absorption of shortwave and longwave radiation by aerosol in the atmosphere. Scattering has a cooling effect, as part of the scattered energy escapes from the atmosphere. Absorption warms the layer in which it occurs. The balance between these two processes depends on aerosol properties, but on average the cooling effects outweigh. Where the second group is concerned, it is the impact of aerosol on cloud formation and in this way on albedo that is assessed. The change in abundance of hydroscoping aerosol can enhance the amounts of droplets in clouds, but their size is usually smaller. Such clouds reflect more solar radiation, with the result that a cooling effect ensues. However the other aerosol – cloud formation processes can lead to warming of the atmosphere. At the moment, all available studies indicate that the net effect of aerosols on clouds is to give cooling of the troposphere. The black carbon effect in turn entails an increase in the albedo of ice or snow by the addition of black carbon, and thus a warming of the climate system. Figure 9 summarises the RF due to aerosol-radiation effects.

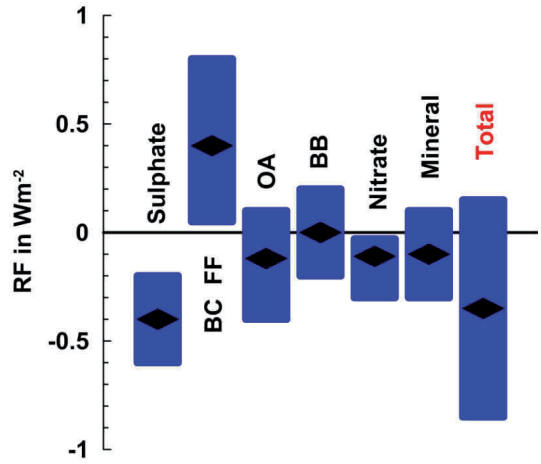

Figure 9. Annual average for RF due to aerosol-radiation effects

Diamonds show the median line, boxes the range to the 5th to 95th percentiles. BC FF is for black carbon from fossil fuels and biofuels, OA for organic aerosol and BB for biomass burning aerosol (data from AR5, IPCC 2013)

Human activity has led to significant changes in land cover. According to the findings of Hurtt *et al.* (2006) the period 1700–2000 saw some 42 to 68% of the global land surface impacted upon by human activities. The most intensive transformations occurred in the mid latitudes of the Northern Hemisphere. These changes impacted upon the radiative balance through a change in urface albedo and latent heat fluxes, but also had other climatic consequences through their modification of the water cycle and river runoff, surface roughness, the emission of dust, snow cover and so on. If these changes entailed deforestation then they also had an impact on GHG concentration. Some of these changes (like the increase in GHG concentration) led to warming, while

others (like higher albedo of crop land and urban surfaces) led to cooling, making the assessment of total RF due to land-use change a more challenging task. Summarising, the net effect of land-use change on RF is seen to be relatively small, being assumed to be of –0.15 (–0.25 – –0.05) Wm^{-2} according to AR5.

NATURAL DRIVERS

For many decades solar irradiance and global temperature moved together (Fig. 10). This allowed opponents of the anthropogenic climate change theory to blame the Sun for temperature increases. However since the end of the 1970s, total solar irradiance has been decreasing, while global temperature have been rising continuously, so the curves are now moving in opposite directions. In fact, the changes in RF due to natural variability of solar irradiance are relatively small, assumed to be at 0.05 (0.00–0.10) Wm^{-2} (IPCC 2013) in 2011.

Contemporary climate change does not manifest itself in relentless warming, being rather superimposed on natural fluctuations – of which the most important arise from ENSO, solar irradiance and variability in atmospheric and oceanic circulation. When natural climate variability is in its warming phase this exacerbates temperature rise. In turn, when in the opposite phase it can slow down or even entirely offset warming for a decade or so (Trenberth, Fasullo 2013).

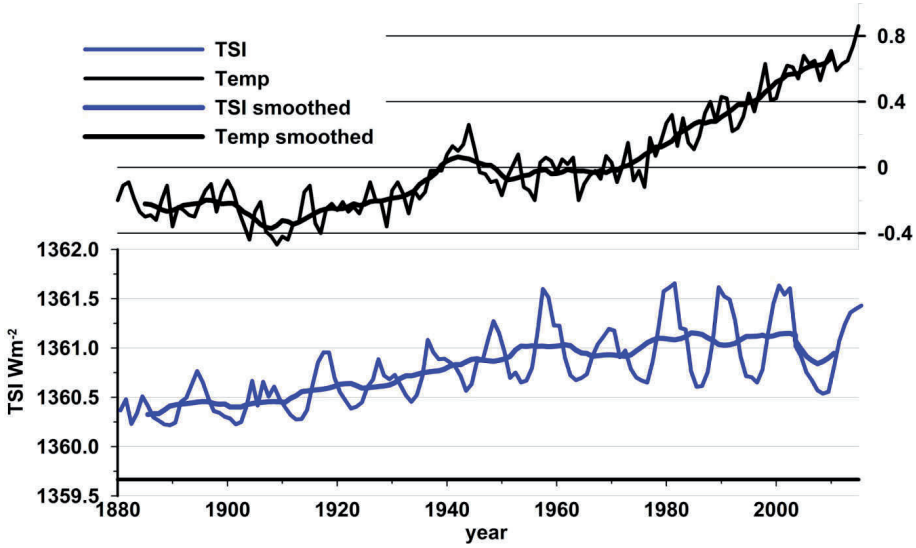

Figure 10. Global Land-Ocean temperature anomalies from the period 1951–1980, based on land data from GHCN-v3 1880-05/2016 and ocean data from ERSST v4 1880-05/2016 (upper graph) and annual values for total solar irradiance in the period 1880–2015 (lower graph, reconstruction based on Naval Research Laboratory Total Solar Irradiance model NRLTSI2, Coddington *et al.* 2015), raw series and 11-year running averages

The most major fluctuations in mean global surface temperature occur with ENSO as a complex effect of direct SST warming in the tropical Pacific, and the delayed effect of changes in atmospheric circulation forced through increased evaporation (Trenberth *et al.* 2002). Figure 11 presents the global mean surface temperature in comparison with the intensity of ENSO events as expressed by the Multivariate ENSO Index (MEI). It is clear that El Niño events correspond very well with the increase in warming, while La Niña events can offset warming for a few years. The impact on the global mean temperature of the two strongest El Niño events (of 1983 and 1998) is compared in Figure 12. The reactions of global mean temperature are very similar, though the mean

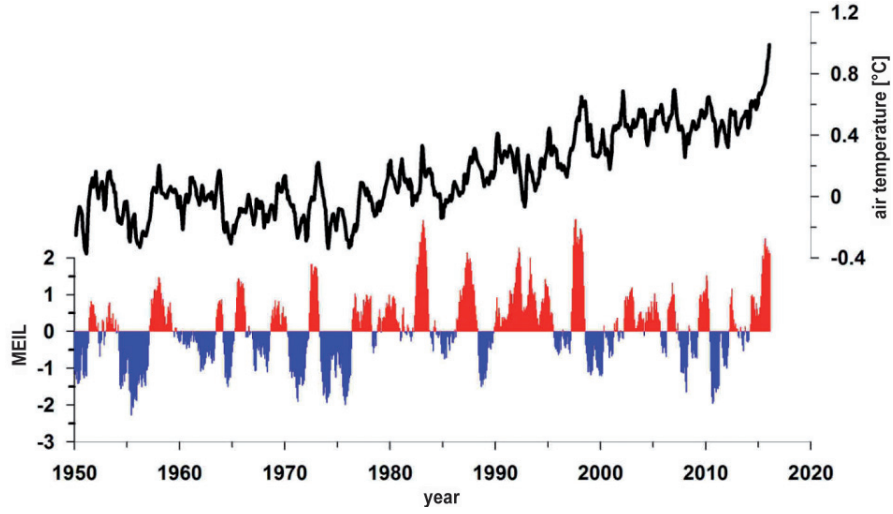

Figure 11. The influence of El-Niño events on global temperature

Upper graph: The HadCRUT4 global mean temperature anomalies as set against the 1961–1990 average values (Morice *et al.* 2012). Lower graph: MEI index showing the El Niño – La Niña fluctuations (El-Niño events in red, La-Niña events in blue). MEI data taken from the Earth System Research Laboratory, www.esrl.noaa.gov/psd/enso/mei/

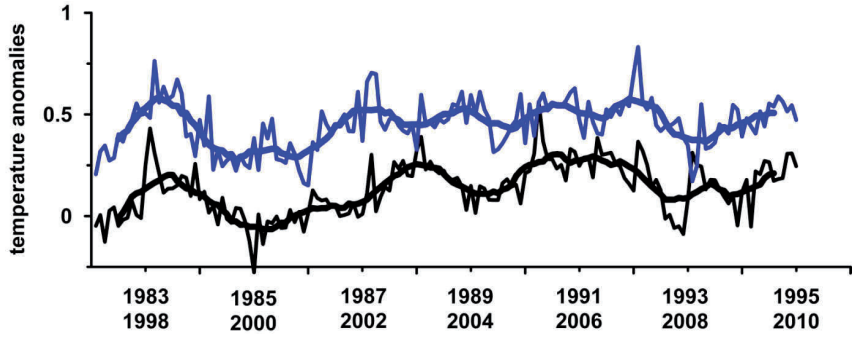

Figure 12. Comparison of HadCRUT4 global mean surface air temperature anomalies (°C) in: 1982–1994 (blue lines) and 1997–2009 (black lines). Monthly values (thin lines) and 11-month running averages (thick lines)

size of departures is about 0.32°C greater in the second period, on account of the temperature increase due to global warming. During an El Niño phase of ENSO the heat comes out of the upper ocean and warms the surface and the atmosphere, whereas during La Niña events the surface fluxes of heat go to the ocean, warming it not only locally, because the heat is redistributed by currents (Trenberth *et al.* 2002).

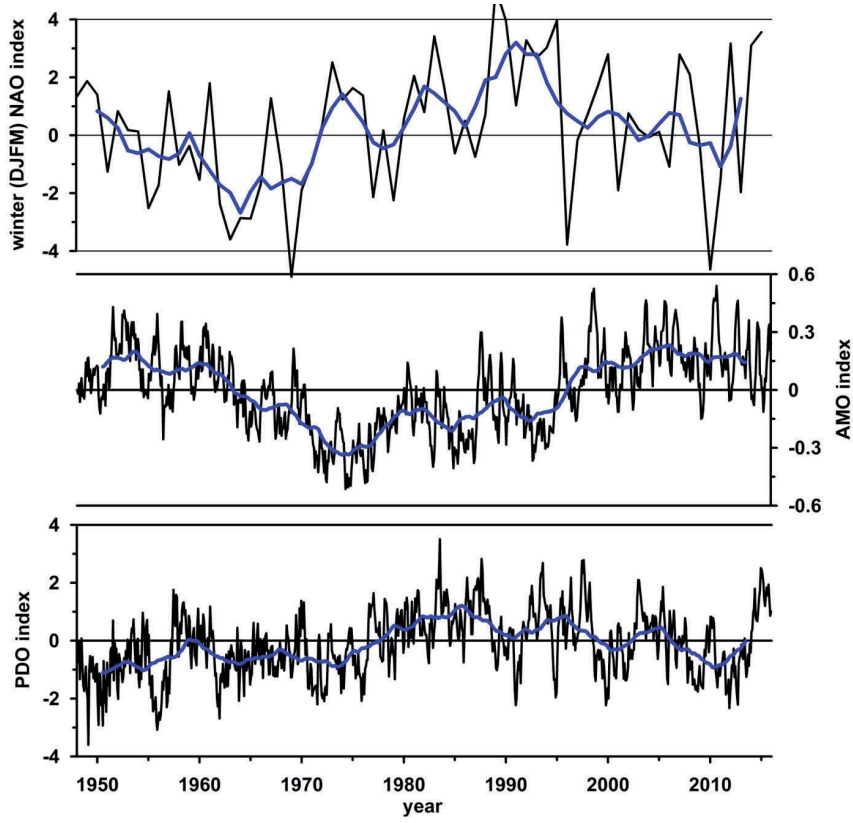

Figure 13. Upper graph: winter NAO index (DJFM) defined by Hurrell (Hurrell and Deser, 2009), annual values and 5-year running averages, middle graph: monthly AMO index (black line) with 61-month running averages (blue) – www.esrl.noaa.gov/psd/data/timeseries/AMO/, lower graph: PDO index monthly values (black line) with 61-month running averages (blue) – Mantua *et al.* 1997, data taken from http://research.jisao.washington.edu/pdo/PDO.latest

The variability of ENSO is sufficient to influence the global mean surface temperature. The impact of decadal oscillations of atmospheric and oceanic circulation is more limited regionally. Among the most important oscillations is the Pacific Decadal Oscillation (PDO), – Figure 13c. It is a recurring pattern of variability in the mid–latitude Pacific Basin north of 20°N. During the warm or positive phase, the eastern part of the ocean warms, while the western becomes cooler. The opposite is true during the negative or cool phase. This pattern significantly affects temperatures over North America, especially its

western part. The North Atlantic Oscillation (NAO), – Figure 13a is the most prominent teleconnection pattern in the Northern Hemisphere (Barnston, Livezey 1987). It manifests itself as a large scale mass alternation between the Subtropical High (the Azores High) and the Polar (or Icelandic) Low (Walker 1924, Wibig 2008). The NAO has a strong influence on weather in winter. During this season in the positive phase of NAO the temperature in all of Europe (away from the south), much of northern Eurasia and the central and western United States is warmer than usual, whereas cooler conditions occur in the northeastern part of the North America, southern Europe and the Northern Pacific (Wanner *et al.* 2001).

PROJECTIONS FOR FUTURE

For future climate projections to be obtained, climate models have to accommodate information about key future climate drivers, mainly future anthropogenic GHG and aerosol emissions and land use. These drivers are forced by economic and population growth in relation to policy on energy and technology, and land use changes, and they can be strongly modified by behavioural factors and lifestyle changes. All are fundamentally unknown, with this being the main reason for future climate projections to be nothing more than scenarios dependent on future development paths.

The 3rd and 4th Assessment Reports made use of the set of scenarios of possible anthropogenic future forcings developed in the Special Report on Emissions Scenarios (SRES 2000). These scenarios were grouped into four families representing different storylines of future development called A1, A2, B1 and B2. The A1 family is divided into three lines according to alternative directions that energy production technologies might take, i.e. intensive fossil fuel use (A1FI), non-fossil energy sources (A1T) and mixed (A1B). The families also differ in their general assumptions as regards demographic change, economic development, trends regarding energy technologies and social interactions. Table 1 shows the future emissions projected under the SRES scenarios.

Table 1. CO_2 concentration in the 21st century as assumed under different SRES scenarios

Year	A1B	A1T	A1FI	A2	B1	B2
2000	369	369	369	369	369	369
2010	391	389	389	390	388	388
2020	420	412	417	417	412	408
2030	454	440	455	451	437	429
2040	491	471	504	490	463	453
2050	532	501	567	532	488	478
2060	572	528	638	580	509	504
2070	611	550	716	635	525	531
2080	649	567	799	698	537	559
2090	685	577	885	771	545	589
2100	717	582	970	856	549	621

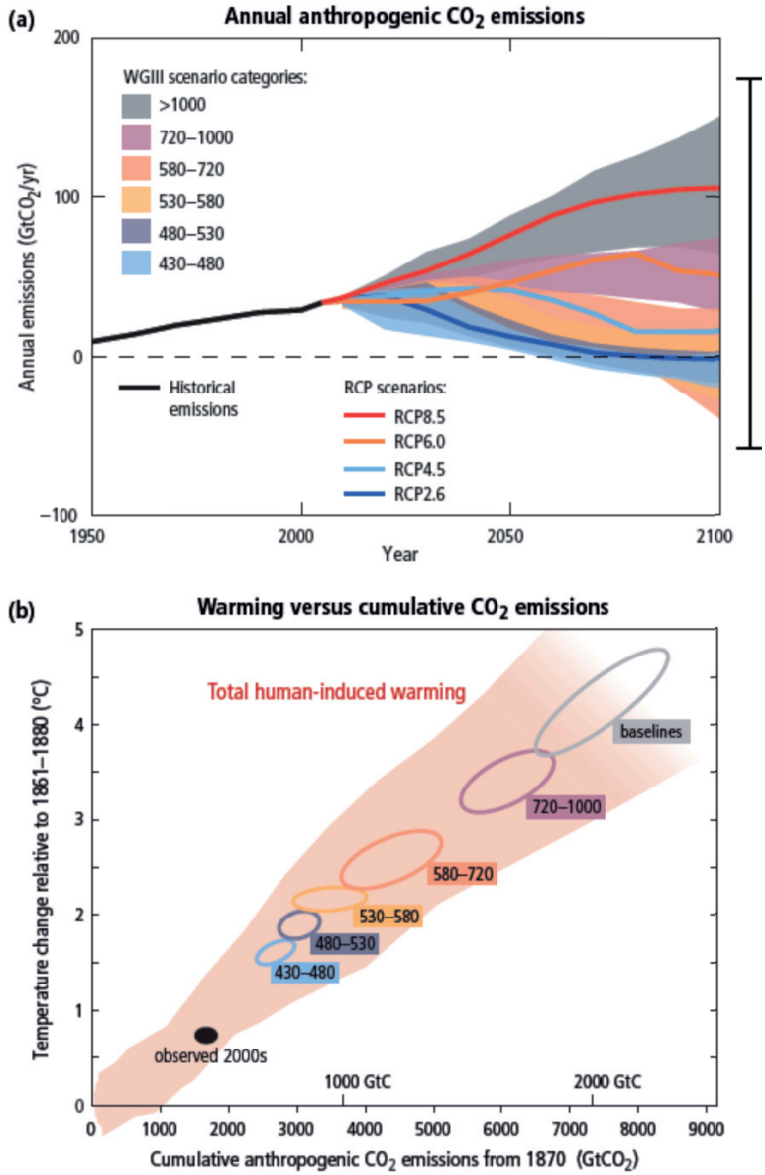

Figure 14. (a) Emissions of carbon dioxide (CO_2) alone in the RCPs (lines) and the associated scenario categories (coloured areas show the 5 to 95% range) used in WG3 AR5 (IPCC, 2014). (b) Global mean surface temperature increase at the time global CO_2 emissions reach a given net cumulation total, plotted as a function of that total, from various lines of evidence. Coloured plume shows the spread of past and future projections. Ellipses show total anthropogenic warming in 2100 versus cumulative CO_2 emissions from 1870 to 2100 from a simple climate model (median climate response) under the scenario categories used in WG3 (Fig. SPM5 from AR5 Synthesis Report IPCC 2014)

For the 5th Assessment Report the possible future development paths were represented by four groups of so called Representative Concentration Pathways (further RCPs) which are future GHG concentration trajectories. RCP2.6, RCP4.5, RCP6 and RCP8.5 are named after possible ranges of radiative forcing values in the year 2100 relative to pre-industrial values (+2.6, +4.5, +6.0, and +8.5 W/m^2, respectively). The RCPs cover a wider range than the SRES scenarios (SRES 2000). In terms of forcing, RCP8.5 is comparable with the SRES A2 and A1FI scenarios, RCP6.0 to B2 and RCP4.5 to B1. The RCP2.6 scenario has no equivalent in SRES (IPCC 2014).

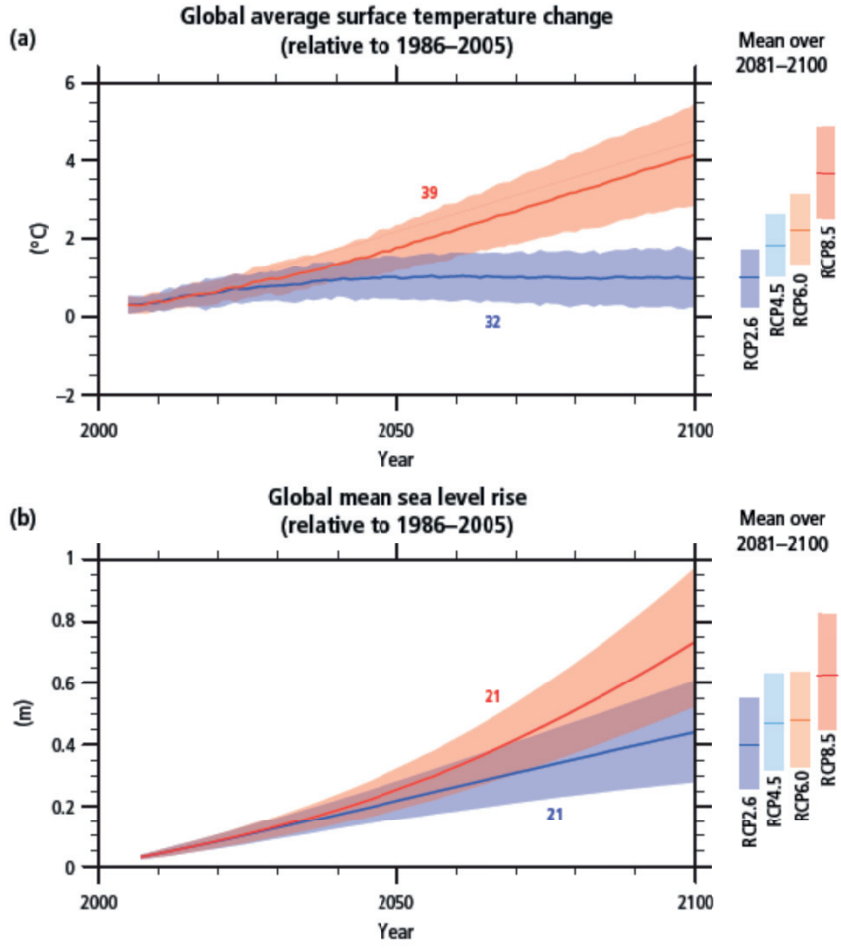

Figure 15. Global average surface temperature change (a) and global mean sea level rise (b) from 2006 to 2100 as determined by multimodel simulations. All changes are relative to 1986–2005. Time series of projections (lines) and a measure of uncertainty (shading) are shown for scenarios RCP2.6 (blue) and RCP8.5 (red). The mean and appropriate uncertainties averaged over 2081–2100 are given for all RCPs as coloured vertical bars at the right hand side of each panel. The number of Coupled Model Intercomparison Project Phase 5 (CMIP5) models used to calculate the multimodel mean is indicated. (Fig. SPM6 from AR5 Syntesis Report – IPCC 2014)

Surface temperature is projected to rise over the 21st century under all considered emission scenarios (IPCC 2014). The increase in global mean surface temperature by the end of the 21st century (2081–2100) relative to the 1986–2005 period is an assessed 1.0 ± 0.7°C for RCP2.6, 1.85 ± 0.75°C for RCP4.5, 2.25 ± 0.85°C for RCP6.0 and 3.7 ± 1.1°C for RCP8.5 (Fig. 15, Tab. 2). Together with the change in mean temperature there will be more hot and fewer cold temperature extremes. Heat waves will occur more frequently and will last longer than today. Extreme high temperatures exceeding today's maxima will be capable of appearing, while extreme cold temperatures will continue to occur occasionally. Extremely hot summers, like the one from 2003 in Western Europe with a mean temperature exceeding the contemporary long-term average by up to five standard deviations will became typical in the middle of the 21st century, but will even be quite cool by the standards of the end of the 21st century (Schär *et al.* 2004).

Table 2. Projected change in global mean surface temperature and global mean sea level rise for the mid- and late-21st century, relative to the 1986–2005 period (after Table 2.1 from Climate Change 2014, Synthesis Report, SYR, IPCC 2014)

Variable	Scenario	2046–2065	2081–2100
Global mean surface temperature change [°C]	RCP2.6	1.0 ± 0.6	1.0 ± 0.7
	RCP4.5	1.4 ± 0.6	1.8 ± 0.7
	RCP6.0	1.3 ± 0.5	2.2 ± 0.9
	RCP8.5	1.0 ± 0.6	3.7 ± 1.1
Sea level change [m]	RCP2.6	0.24 [0.17–0.32]	0.40 [0.26–0.55]
	RCP4.5	0.26 [0.19–0.33]	0.47 [0.32–0.63]
	RCP6.0	0.25 [0.18–0.32]	0.48 [0.33–0.63]
	RCP8.5	0.30 [0.22–0.38]	0.63 [0.45–0.82]

The spatial pattern characterising temperature trends (Fig. 16a) shows that warming will not be uniform over the whole Earth. Rather, the most marked warming is anticipated for the northern latitudes of the Northern Hemisphere – as result of the positive feedback from sea ice melting. The warming over the land will be stronger than over the ocean and stronger than the global mean.

Warming will cause changes in precipitation patterns across the globe. These changes will be even less uniform than the temperature changes. For some regions, for example in high latitudes and in the Equatorial Pacific, an increase in annual precipitation is predicted. In dry regions in mid-latitudes and the Tropics a decrease in precipitation is foreseen, whereas in wet mid-latitudes the precipitation totals should increase. It means that what are today wet regions will become more wet, while today's dry regions become more dry (Fig. 16b). Even in regions where precipitation will not increase, the intensity of given falls of rain is projected to increase. Such tendencies are already observable (Lenderink, van Mejigaard 2008) and are expected to intensify in the future (IPCC 2013). This is due to a warmer atmosphere being able to contain more water vapour.

A strong temperature rise together with only a small increase – or even a decrease – in precipitation totals is bound to be associated with a significant increase in evapotranspiration. This means that a water deficit may intensify in regions which are dry today, while also appearing in regions in which the water surplus is scant at the moment. The intensification and extension of aridity will foster forest fires in many areas of the globe, as well as limiting acreage.

The warming of the ocean surface will continue. This is likely to impact upon ocean circulation. It is likely that the Atlantic Meridional Overturning Oscillation (AMOC) will weaken. However the closure of AMOC is not expected in the 21st century. Sea surface warming will probably cause the further melting of sea ice in the Northern Hemisphere. And by the second half of the 21st century, the Arctic Ocean is expected to be ice-free during late summer.

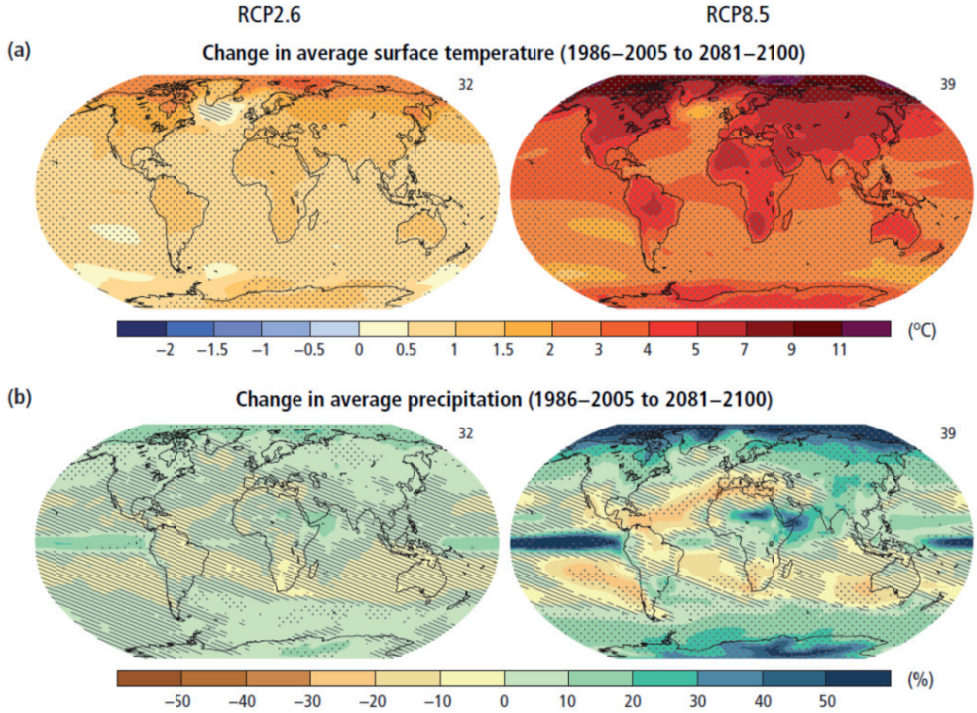

Figure 16. Coupled Model Intercomparison Project Phase 5 (CMIP5) multi-model mean projections (i.e., the average of the model projections available) for the 2081–2100 period under the RCP2.6 (left) and RCP8.5 (right) scenarios for (a) change in annual mean surface temperature and (b) change in annual mean precipitation, in percentages. Changes are shown relative to the 1986–2005 period. The number of CMIP5 models used to calculate the multi-model mean is indicated in the upper right corner of each panel. Stippling (dots) on (a) and (b) indicates regions in which the projected change is large compared with natural internal variability (i.e. greater than two standard deviations for the internal variability in 20-year means), and where 90% of the models agree on the sign of the change. Hatching (diagonal lines) on (a) and (b) shows regions in which the projected change is less than one standard deviation about the natural internal variability in 20-year means (after Fig. 2.2 from SYR – IPCC 2014b)

Warming will also cause melting of ice on Greenland and in the Antarctic. As a result of the melting, and the attendant warming of ocean water, sea level should rise. The projections for of this increase through to the end of the 21st century vary from 24 cm in the RCP2.6 scenario to more than 60 cm under RCP8.5 (Tab. 2).

Projected climate changes will have numerous environmental consequences, including the flooding of coastal areas, shifts in vegetation zones, conditions of water deficit in numerous areas (but also floods in others), ocean acidification, the extinction of many species of fauna and flora, and many others. A majority of these changes are to be observed today, but they will intensify in future. It is impossible to predict all of them at the moment, but surely they will change ecosystems, human lives and economies in a tremendous way.

REFERENCES

Andrews T., Ringer M., Doutriaux-Boucher M., Webb M., Collins W., 2012, *Sensitivity of an Earth system climate model to idealized radiative forcing*, Geophys. Res. Lett., 39, L10702.

Archer D., Rahmstorf S., 2010, *The climate crisis. An introductory guide to climate change*, Cambridge University Press, New York, pp. 249.

Barnston A.G., Livezey R.E., 1987, *Classification, seasonality and persistence of low-frequency atmospheric circulation patterns*, Mon. Wea. Rev., 115, 1083–1126.

Coddington O., Lean J.L., Pilewskie P., Snow M., Lindholm D., 2015, *A solar irradiance climate data record*, Bull. American Meteorological Soc., DOI: 10.1175/BAMS-D-14-00265.12.

Dlugokencky E.J., Lang P.M., Crotwell A.M., Masarie K.A., Crotwell M.J., 2015, Atmospheric Methane Dry Air Mole Fractions from the NOAA ESRL Carbon Cycle Cooperative Global Air Sampling Network, 1983–2014, Version: 2015-08-03, Path: ftp://aftp.cmdl.noaa.gov/data/trace_gases/ch4/flask/surface/.

Enfield D.B., Mestas-Nunez A.M., Trimble P.J., 2001, *The Atlantic Multidecadal Oscillation and its relationship to rainfall and river flows in the continental U.S.*, Geophys. Res. Lett., 28, 2077–2080.

Hansen J., Ruedy R., Sato M., Lo K., 2010, *Global surface temperature change*, *Rev. Geophys.*, 48, RG4004, DOI: 10.1029/2010RG000345.

Henson R., 2008, *The Rough Guide to Climate Change*, Second edition, Rough Guides, Ltd, New York, USA.

Hurrell J.W., Deser C., 2009, *North Atlantic climate variability: The role of the North Atlantic Oscillation*, J. Mar.Syst., 78, 28–41.

Hurtt G.C., Frolking S., Fearon M.G., Moore B., Sherliakova E., Malysher S., Pacola S.W., Houghton R.A., 2006, *The underpinning of land-use history: Three centuries of global gridded land-use transitions, wood-harvest activity, and resulting secondary lands*, Global Change Biol., 12, 1208–1229.

IPCC, 2013, *Climate Change 2013: The Physical Science Basis*. Contribution of Working Group I to the Fifth Assessment Report of the Intergovernmental Panel on Climate Change, Stocker T.F., Qion D., Plattner G-K., Tgnor M., Allen S.K., Boschung J., Nauels A., Xia Y.,

Bex V., Midgley P.M. (eds.), Cambridge University Press, Cambridge, United Kingdom and New York, NY, USA, 1535 pp.

IPCC, 2014, *Climate Change 2014: Synthesis Report*. Contribution of Working Groups I, II and III to the Fifth Assessment Report of the Intergovernmental Panel on Climate Change, Core Writing Team, R.K. Pachauri, L.A. Meyer (eds), IPCC, Geneva, Switzerland, 151 pp.

Kopp G., Krivova N., Lean J., and Wu C.J., 2016, *The Impact of the Revised Sunspot Record on Solar Irradiance Reconstructions*, Solar Physics, DOI: 10.1007/s11207-016-0853-x

Lenderink G., van Mejigaard E., 2008, *Increase in hourly precipitation extreme beyond expectation from temperature changes*, Nat. Geosci., 1, 511–514.

Mantua N.J., Hare S.R., Zhang Y., Wallace J.M., Francis R.C., 1997, *A Pacific interdecadal climate oscillation with impacts on salmon production*, Bull of Am. Met. Soc., 78, 1069–1079.

Morice C.P., Kennedy J.J., Rayner N.A., Jones P.D., 2012, *Quantifying uncertainties in global and regional temperature change using an ensemble of observational estimates: The HadCRUT4 data set*, Journal of Geophysical Research, 117, D08101, DOI: 10.1029/2011JD017187.

Schär C., Vidale P.L., Lüthi D., Frei C., Häberli V., Liniger M.A., Appenzeller C., 2004, *The role of increasing temperature variability in European summer heatwaves*, Nature, 427, 332–336.

Trenberth K.E, Fasullo J.T., 2013, *An apparent hiatus in global warming?* Earth's Future, 1, 19–32, DOI: 10.1002/2013EF000165.

Trenberth K.E., Caron J.M., Stepaniak D.P., Worley S., 2002, *Evolution of El Niño – Southern Oscillation and global atmospheric surface temperatures*, Journal of Geophysical Research, 107, D8, DOI: 10.1029/2000JD000298.

Walker G.T., 1924, *Correlation in seasonal variation of weather*, IX Mem. Ind. Met. Dept., 25, 275–332.

Wanner H.S., Brönnimann S., Casty C., Gyalistras D., Luterbacher J., Schmutz C., Stephenson D.B., Xoplaki E., 2001, *North Atlantic Oscillation – concepts and studies*, Survey geophys, 22, 321–381.

Wibig J., 2008, *North Atlantic Oscillation and Arctic Oscillation*, [in:] Assessment of Climate Change for the Baltic Sea basin, Springer Berlin, Germany, 479–449.

Zhang J., 2007, *Increasing Antarctic Sea Ice under Warming Atmospheric and Oceanic Conditions*, Journal of Climate, 20, 2515–2529.